WARSAW UNIVERSITY OF TECHNOLOGY Index 351733
FACULTY OF CIVIL ENGINEERING
COMMITTEE FOR CIVIL AND WATER ENGINEERING
POLISH ACADEMY OF SCIENCES ISSN 1230-2945
DOI: 10.24425/ace.2025.155093
ARCHIVES OF CIVIL ENGINEERING
Vol. LXXI ISSUE 3 2025
pp. 181 –198

Research paper

EN 1992-1-1:2023 – a new look at the issue of punching shear design

Michał Gołdyn[1], Adam Michalak[2]

Abstract: The paper presents a comprehensive evaluation of the revised punching shear design methodology introduced in the new edition of Eurocode 2 (EN 1992-1-1:2023), with particular emphasis on improvements derived from the Critical Shear Crack Theory (CSCT). Previous empirical methods were substituted with a mechanical model formulated as closed-form expressions. The key revisions include a redefined control perimeter located at $0.5d_v$ from the column face (instead of $2d$), harmonization of design approaches for slabs and foundations, revised definitions of effective depths, differentiated contributions of concrete and shear reinforcement to punching shear resistance and the explicit consideration of aggregate composition. The paper also discusses the improved method for accounting for non-uniform shear stress distribution, which offers better agreement with experimental observations and reduces the conservatism and inconsistency associated with previous Eurocode provisions. The new procedure was validated against experimental results from over 300 slab tests, showing average experimental-to-predicted load ratios (V_{exp}/V_{calc}) of 1.10 and 1.20 for slabs without and with shear reinforcement, respectively, with consistent accuracy across a wide range of parameters. The analysis presented in the paper showed that the predictions of the new standard tend to be closer to the experimental ones and provided a better estimate of punching capacity compared to previous approaches ($V_{exp}/V_{calc} \approx 1.22$, COV = 7%). It should be emphasized that the predictions proved to be safe, even though the reinforcement in certain elements did not fully comply with design specifications regarding spacing and the number of perimeters. Moreover, a comparable level of agreement between the experimental and calculated load carrying capacities was observed for both axially and eccentrically loaded elements, which confirmed the validity of the new procedure for determining the effect of the unbalanced bending moment.

Keywords: punching shear, RC slab, control perimeter, shear reinforcement, Eurocode 2

[1]PhD., DSc. Eng., Lodz University of Technology, Faculty of Civil Engineering, Architecture and Environmental Engineering, al. Politechniki 6, 93-590 Lodz, Poland, e-mail: michal.goldyn@p.lodz.pl, ORCID: 0000-0002-7791-1940

[2]MSc. Eng., Lodz University of Technology, International Doctoral School, al. Politechniki 6, 93-590 Lodz, Poland, e-mail: adam.michalak@dokt.p.lodz.pl, ORCID: 0009-0001-2504-5964

1. Introduction

The new generation of Eurocodes is intended to be a more comprehensive, updated and technically advanced set of guidelines that reflect the latest developments in materials, construction technology, sustainability and climate change risks. The new edition of Eurocode 2 (EN 1992-1-1:2023) has brought many changes to the design of reinforced concrete structures. The issue of punching shear is still relevant, as shown by experimental studies and analytical research conducted in numerous research centres [1–5]. The principles for the load-carrying capacity of the support zones of flat slabs have been significantly expanded and made more detailed with respect to the previous edition of the standard. The standard includes the latest findings from experimental research and analytical work carried out in various European centres [6–14]. The design procedure is based on the Critical Shear Crack Theory (CSCT), developed by Muttoni et al. [15, 16], described in more detail in [17, 18], among others. The punching shear carrying capacity is analytically defined as the intersection of the load-rotation relationship of the slab-column connection, describing the flexural response of the slab resulting from the applied shear force, and the failure criterion, indicating the maximum shear force associated with a given state of deformations [15, 19].

Considering the postulate of simplifying design regulations, the concept of successive levels of approximation of the slab rotation, introduced in the pre-norm *fib* Model Code 2010 [20], was abandoned in favour of consistent closed-form equations to contribute to the ease of use of the standard. The detailed approach is left for the evaluation of the existing structures (Annex I [21]). The following sections discuss the most important changes and their implications on the design process.

2. Design principles

2.1. Important changes in the punching shear design

The most important changes in the punching shear design procedure include:

- change in the location of the basic control perimeter from $2d$ to $0.5d_{\mathrm{v}}$ from the edge of the supporting area; the location of the basic control perimeter is thus the same as assumed in the Swiss SIA 262 [22] or the American ACI 318-25 [23] standards;
- unification of the provisions for slender slabs and foundations (the iterative approach was abandoned), assuming that in both cases the critical shear crack forms at an angle of 45°; this assumption applies to all considered control sections – thus, among others, the basic and external control sections;
- differentiation of the effective depths considered in the flexural (d) and punching shear analyses (d_{v} and $d_{\mathrm{v,out}}$) – see Figure 1; the effective depth $d_{\mathrm{v,out}}$ was related at the same time to the type of the shear reinforcement, which influences the formation mechanism of diagonal cracks outside the shear-reinforced area and accounts for the possibility of delamination in compression surface;

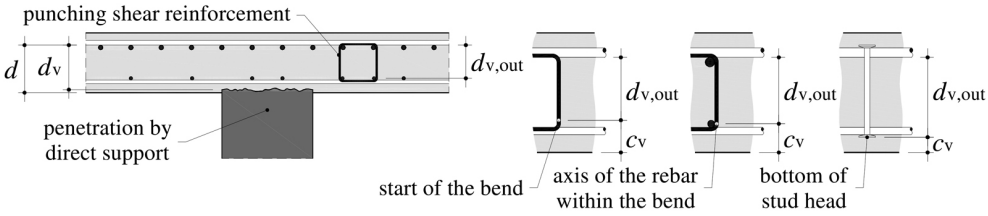

Fig. 1. Definition of the effective depths in the punching shear analysis

– inclusion of the aggregate composition (aggregate particle size), affecting the profile of the failure surface and determining the mechanism of aggregate interlock;
– consideration of the variable contribution of concrete and shear reinforcement to thepunching shear resistance;
– extension of the list of punching shear reinforcement that can be designed in accordance with the code provisions to include double-headed studs; formerly they had to be designed in accordance with the relevant European Technical Approvals (ETA);
– clarification of the guidelines for placing the elements of shear reinforcement, including the formulation of separate rules for slender slabs and foundations.

2.2. Slabs without shear reinforcement

The punching shear load carrying capacity of slabs without transverse reinforcement is defined as the intersection of the curve describing the failure criterion and the load–rotation response function characterizing slab behaviour under load – see also Fig. 6a. Introducing some simplifications [24, 25], including the assumption that the effective depth $d = d_v$ and any effects associated with non-uniform distribution of shear stress on the control perimeter will be taken into account when estimating the shear stress τ_{Ed} (by a factor $\beta_e \geq 1$) and also assuming location of the line of zero radial moment $a_p = 8d$, a function describing the punching shear resistance in a form similar to that used in the existing Eurocode 2 [26] is obtained

$$\tau_{\mathrm{Rd,c}} = \frac{0.6}{\gamma_v} k_{\mathrm{pb}} \sqrt[3]{100 \rho_l f_{\mathrm{ck}} \frac{d_{\mathrm{dg}}}{d_v}} \leq \frac{0.5}{\gamma_v} \sqrt{f_{\mathrm{ck}}} \tag{2.1}$$

where: γ_v – partial safety factor for shear related capacity ($\gamma_v = 1.4$), k_{pb} – shear strength increase factor, ρ_l – longitudinal reinforcement ratio, f_{ck} – concrete compressive strength, d_{dg} – parameter describing the failure zone roughness ($d_{\mathrm{dg}} = d_g + 16$ mm), d_g – smallest value of the upper sieve size for the coarsest fraction of aggregates used, d_v – shear resisting effective depth.

The coefficient k_{pb} appearing in the expression (2.1) accounts for the strength enhancement due to the shear field gradient in the control section and represents a smooth transition between one- and two-way shear [16]. It considers the relationship between the shear force V_{Ed} and the bending moment acting in the width of the support strip m_{Ed}. Taking into account the function

describing the relationship between the lengths of the basic perimeter and perimeter of the support region, the parameter k_{pb} can be expressed as follows

$$k_{\mathrm{pb}} = \sqrt{5\frac{d_{\mathrm{v}}}{b_{0,5}}\mu_{\mathrm{p}}} = \sqrt{5\frac{d_{\mathrm{v}}}{b_{0,5}} \cdot \frac{8}{\pi d_{\mathrm{v}}}(b_{0,5} - b_0)} \cong 3.6\sqrt{1 - \frac{b_0}{b_{0,5}}} \tag{2.2}$$

where: b_0 – length of control perimeter at face of supporting area, $b_{0,5}$ length of control perimeter at a distance of $0.5d_{\mathrm{v}}$ from column edge, and k_{pb} restricted to 2.5, reflecting the limitation of shear resistance for very small supporting areas.

Figure 2 compares the punching shear resistance according to the existing ($v_{\mathrm{Rd,c}}$) and new edition of the standard ($\tau_{\mathrm{Rd,c}}$).

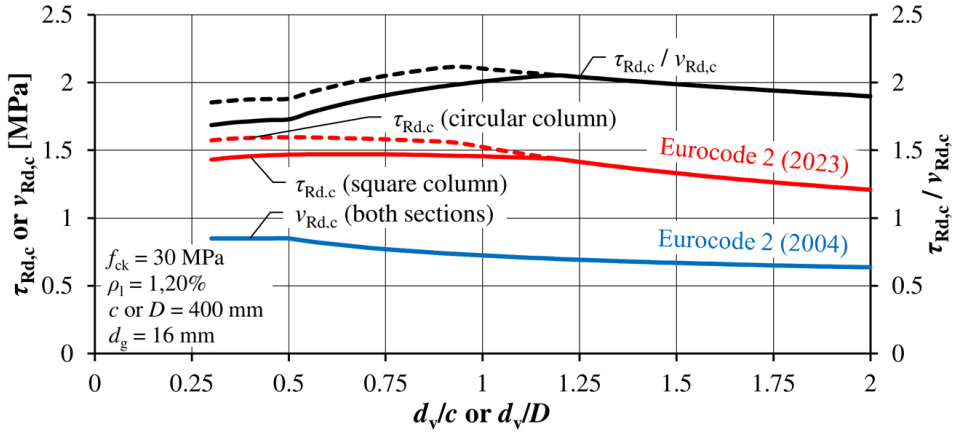

Fig. 2. Comparison between punching shear resistance according to existing and the new approach

Changing the position of the basic control perimeter required adjusting the stresses, which are about 70÷100% higher. In contrast to the previous Eurocode 2, which only accounted for the effect of slab thickness by means of a scale effects factor, in the range characterizing typical slender slabs, an increase in ultimate stresses accompanying an increase in the d_{v}/c (or d_{v}/D) ratio can be observed. Only in the case of thicker slabs does the upper limit of the k_{pb} factor become decisive (with $d_{\mathrm{v}}/D = 1$ and $d_{\mathrm{v}}/c = 1.2$), a decrease in the $\tau_{\mathrm{Rd,c}}/v_{\mathrm{Rd,c}}$ ratio is observed.

Figure 3 compares the punching shear capacities of flat slabs from concrete C30/37 (f_{ck} = 30 MPa), characterized by a reinforcement ratio $\rho_l = 1.20\%$, depending on the relation between the effective depth and the column dimension (width c or diameter D), in light of the existing [26] and the new edition of Eurocode 2 [21]. In the case of a square column, the load capacities resulting from the new procedure are lower – in the range of $d_{\mathrm{v}}/c = 0.5 \div 2$ by about 5÷30%. The difference between two design approaches increases as the d_{v}/c ratio increases. Therefore, lower punching shear capacities should be expected for thicker (less slender) slabs such as transfer slabs. For a column with a circular cross-section, the load carrying capacity

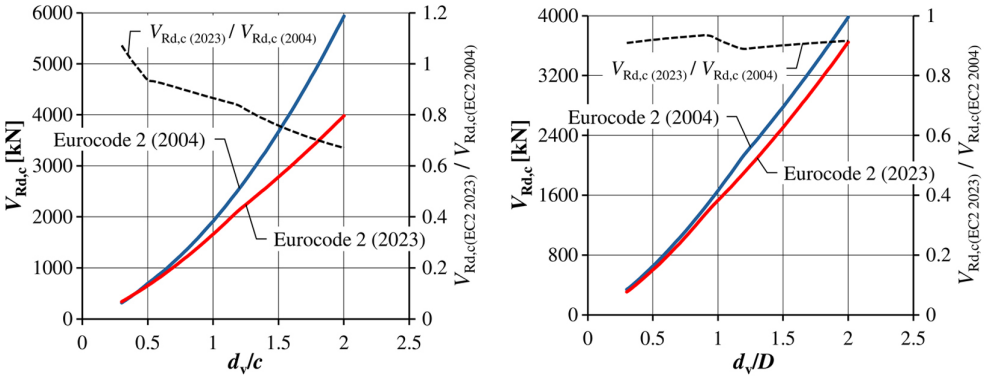

Fig. 3. Comparison of the punching shear carrying capacities according to Eurocode 2 edition 2004 [26] and 2023 [21], with respect to effective depth to column size aspect ratio: (a) square, (b) circular column

according to the new standard [21] is about 8÷10% lower, regardless of the d_v/D ratio. The reasons for the differences are primarily to be found in the association of punching shear resistance with shape and size of the supporting area as well as effective depth of the slab, which are captured by the parameter k_{pb}.

2.3. Effect of the unbalanced bending moment

A very important and desirable modification is the revision of the method for calculating the increasing factor β, which takes into account the concentration of shear stresses due to the action of the unbalanced bending moment transferred from the slab to the column. This coefficient is a design simplification that increases the punching force V_{Ed} when determining the shear stress τ_{Ed}. Based on a systematic analysis conducted using the finite element method, including structural systems characterized by varying floor spans and thicknesses as well as column shapes and sizes, Vollum et al. [13] specified the relationship between maximum shear stresses and average stresses along the length of the reduced perimeter. The results obtained made it possible to formulate the following relationship

$$\beta_e = 1 + 1.1\frac{e_b}{b_b} \geq 1.05 \tag{2.3}$$

where: e_b – the eccentricity of the resultant of shear force with respect to the centroid of the control perimeter, b_b – geometric mean of the minimum and maximum overall widths of the control perimeter.

Figure 4 compares the increasing coefficients β, characterizing the edge and corner supports. The analyses assumed a square column with a side length of $c = 400$ mm, adopting a rather wide range of relative eccentricities $e/c = 1.0 \div 1.8$, covering most cases encountered in practice. It can be clearly seen that the predictions of the existing standard EN 1992-1-1:2004 [26]

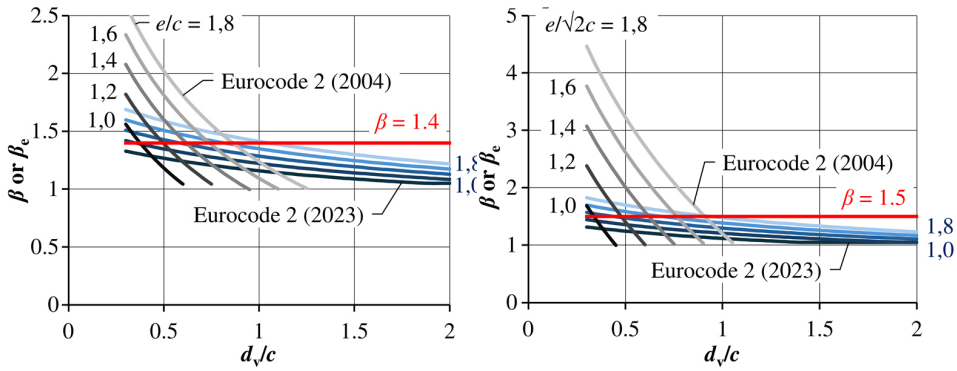

Fig. 4. Comparison between coefficients including effect of the concentration of shear forces in the case of: (a) edge, (b) corner column-and-slab connections

lead to a significant variation in β coefficients, reaching about 2.5 and even 4.5 for edge and corner supports, respectively. In the case of flat slabs of common thickness ($d_v/c \approx 0.4 \div 0.5$) and eccentricity $e > 1.2c$, typical for edge connections in slab-and-column systems with a uniform support grid in both directions, β coefficients exceeding, sometimes significantly (even by 40%), the value of $\beta = 1.40$ assumed as safe simplification. Similar observations apply to corner supports, where the achieved values of β coefficients are even higher and significantly deviate from the constant value of $\beta = 1.50$, even by $35 \div 100\%$. These discrepancies raised serious doubts about the validity of the predictions of the standard procedure, as pointed out, among others, in the papers of Gołdyn and Urban [27, 28], since they did not reflect the results of experimental investigations, leading to an underestimation of the punching shear capacity – on average, even by about 50%.

The values of the β_e coefficients derived from equation (2.3) are much more consistent. Even with relatively high eccentricities $e = 1.8c$, reflecting the effect of the high unbalanced bending moment, the coefficients β_e are only about 20% higher than the constant values recommended as a simplification in stiffened structures with a uniform support grid. At the same time, the expression (2.3) is considerably simpler to use, since the cumbersome determination of the perimeter coefficient W_1 with respect to the axis of the net bending moment is not required, as was the case in the procedure [26].

The effect of the aforementioned changes in the determination of punching shear resistance as well as the effect of the concentration of shear stress in the control section was analysed on the example of edge columns with a section of 400×400 mm, connected with a slab of thickness $h = 150 \div 330$ mm, made of concrete class C30/37. A constant relative eccentricity e/c was assumed. For floor slabs of typical thicknesses ($d_v/c = 0.4 \div 0.5$), the load capacities resulting from the predictions of the new standard are $5 \div 20\%$ and even $20 \div 50\%$ higher for edge and corner columns, respectively – see Fig. 5. This is primarily a result of changes in the way the β coefficient is determined, especially for corner columns.

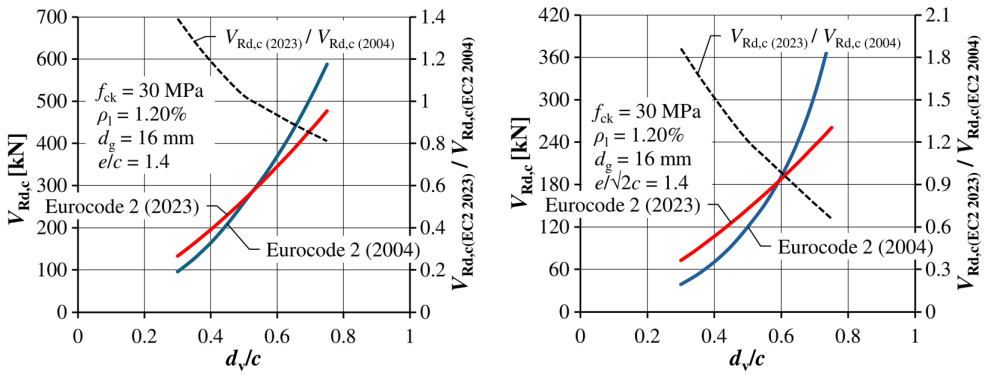

Fig. 5. Comparison of the punching shear carrying capacities according to existing [26] and the new edition [21] of Eurocode 2 in the case of: (a) edge, (b) corner column-and-slab connections

2.4. Contribution of shear reinforcement

The contribution of shear reinforcement allows to increase the punching shear capacity of slabs, which is mainly due to the limitation of the width of diagonal cracks by intersecting bars (vertical or bent). From the failure criterion presented previously, it follows that the punching shear capacity of a slab without transverse reinforcement is a function of deformation, represented by the rotation angle ψ. Considering the descending branch of the exponential failure criterion and adopting $\eta_c = V_{R,c}/V_E$ ($V_{R,c}$ is the punching shear capacity of the slab without shear reinforcement and V_E is the shear force), the contribution of concrete to the punching resistance can be written as $V_{Rc,E} = V_{R,c} \cdot \eta_c$ [8]. Including the relationship between width of the diagonal crack (which depends on the rotation angle) and the stress activated in the shear reinforcement, taking into account the simplified stress-rotation relationship, the equation describing the punching shear resistance of shear-reinforced slab can be obtained

$$\tau_{Rd,cs} = \eta_c \cdot \tau_{Rd,c} + \eta_s \cdot \rho_{sw} \cdot f_{ywd} \geq \rho_{sw} \cdot f_{ywd} \tag{2.4}$$

where: $\tau_{Rd,c}$ – punching shear resistance of slab without shear reinforcement, see Eq. (2.1), η_c – the concrete contribution reduction factor, η_s – the shear reinforcement contribution reduction factor, f_{ywd} – yield strength of the shear reinforcement, ρ_{sw} – shear reinforcement ratio, including cross-sectional area of the elements and its spacing in radial and tangential direction [$\rho_{sw} = A_{sw}/(s_r \cdot s_t)$].

Figure 6a illustrates the punching resistance resulting from the contribution of concrete (grey area) and transverse reinforcement (red area). Unlike the procedure [26], the new standard assumes a variable contribution of concrete and reinforcement to the punching resistance of a slab with transverse reinforcement. The procedure [26] implied a constant concrete contribution, which was 75% of the punching resistance of a slab without shear reinforcement. The change in philosophy is explained by the need to reflect the physical behaviour of reinforced concrete slabs. As deformation and associated cracking increase, a decreasing contribution

of concrete is to be expected, while the contribution of reinforcement increases. The upper limit of the ratio $\eta_s = 0.8$ is based on the assumption that only a portion of the punching shear reinforcement can be activated and yield. Figure 6b shows the contribution of concrete and reinforcement as a function of the shear stress to punching shear resistance ratio $\tau_{Ed}/\tau_{Rd,c}$ (level of punching shear resistance exceedance). In the range $\tau_{Ed}/\tau_{Rd,c} = 1.0 \div 1.8$, resulting from the maximum punching shear resistance, the contribution of concrete varies nonlinearly from 1.0 to about 0.55. The value $\eta_c = 0.75$, corresponding to the previous approach [26], was obtained at $\tau_{Ed}/\tau_{Rd,c} = 1.35$, which corresponds to a moderate level of punching shear resistance utilization.

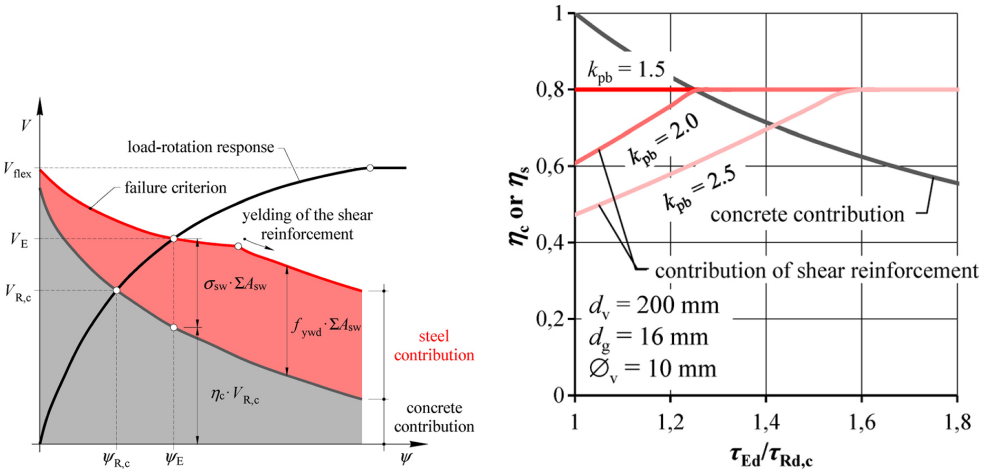

Fig. 6. Contribution of concrete and shear reinforcement on punching shear resistance: a) impact on failure criterion, b) effect of the utilization of shear capacity

By determining the maximum punching shear capacity, a number of parameters were analysed and as the most important were indicated [29]: the type of punching shear reinforcement used, which determines, among other things, the anchorage conditions and the effectiveness in limiting the development of concrete cracking at the same time, the size of the supporting area, and the distribution of the punching shear reinforcement. As before, the maximum punching shear capacity is expressed as a multiple of the punching shear resistance of slab without shear reinforcement

$$\tau_{Rd,max} = \eta_{sys} \cdot \tau_{Rd,c} = \left(\eta_{sys,0} + 0.63\sqrt[4]{b_0/d_v}\right) \cdot \tau_{Rd,c} \tag{2.5}$$

where: $\eta_{sys,0}$ – coefficient dependent on type of punching shear reinforcement (0.70 for headed studs and 0.50 for stirrups and bent-up bars), b_0 – perimeter of the supporting area, d_v – shear resisting effective depth.

In contrast to the previous approach of Eurocode 2 [26] as well as the European technical approvals [30], a constant value for the coefficient expressing the maximum shear resistance capacity was abandoned. Figure 7 shows the variation of the parameter η_{sys} as a function of the

relative perimeter of the supporting zone. In the range of effective depths typical for slender slabs (d_v = 160 ÷ 260 mm), this coefficient is in the range of 1.5 ÷ 1.6 for stirrups. Thus, it is close to the limit value k_{max} = 1.5 introduced to the standard [26] in 2014. However, in the case of double-headed studs higher by about 15% punching shear resistance can be obtained. At the same time the coefficient η_{sys} assumes values lower by about 10 ÷ 15% in relation to the k_{max} limit value adopted in ETA.

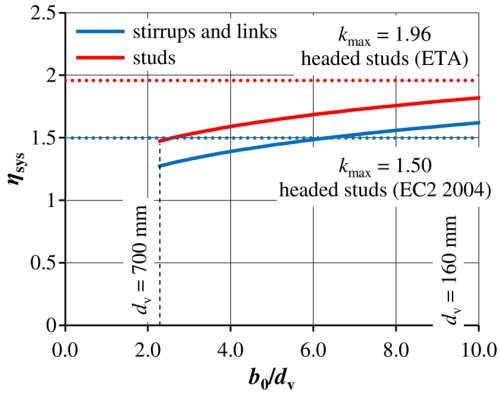

Fig. 7. Coefficient expressing the maximum punching shear resistance, depending on the size of the supporting area

When considering the load capacity outside the area of shear reinforcement, the reduced effective depth $d_{v,out}$ depending on the reinforcement installed is taken into account (see Figure 1). Assuming that the punching shear resistance associated with the outer control section $b_{0,5,out}$ is equal to the required resistance associated with the basic control section ($\tau_{Rd,out} = \tau_{Rd,cs}$), a relation describing the required length of the external control perimeter (excluding failure outside the shear-reinforced area) can be derived

$$k_{pb,out}\tau_{Rd,c} \cdot b_{0,5,out}d_{v,out} = k_{pb}\tau_{Ed} \cdot b_{0,5}d_v \Rightarrow \frac{b_{0,5,out}}{b_{0,5}}\frac{k_{pb,out}}{k_{pb}} = \frac{\tau_{Ed}}{\tau_{Rd,c}} \cdot \frac{d_v}{d_{v,out}}$$

$$\Rightarrow \frac{b_{0,5,out}}{b_{0,5}}\sqrt{\frac{b_{0,5}}{b_{0,5,out}}} = \eta_c\frac{d_v}{d_{v,out}} \tag{2.6}$$

$$b_{0,5,out} = b_{0,5}\left(\frac{1}{\eta_c}\frac{d_v}{d_{v,out}}\right)^2$$

where: $b_{0,5}$ – length of the basic control perimeter, η_c – concrete contribution reduction factor equal to $\tau_{Rd,c}/\tau_{Ed}$, d_v, $d_{v,out}$ – shear resisting effective depths (see Fig. 1).

Figure 8 shows the relationship between the relative shear stress $\tau_{Ed}/\tau_{Rd,c}$ and the required length of the outer control perimeter, which can be up to several times the length of the base perimeter $b_{0.5}$, while the type of shear reinforcement used is also important. The length of the outer perimeter directly affects the required range (number of perimeters) of the punching shear reinforcement, since the last perimeter should be at a distance of less than $0.5d_{v,out}$

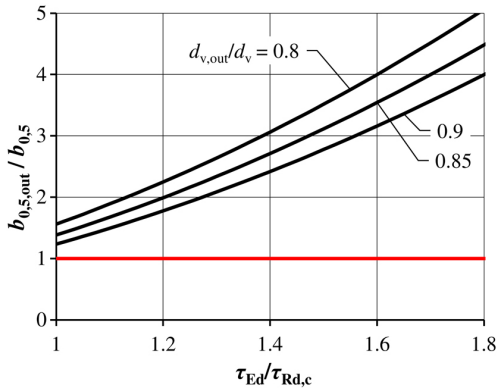

Fig. 8. Required length of the external control perimeter depending on the relative resistance deficit of the slab without shear reinforcement

from the $b_{0,5out}$ perimeter. As demonstrated in [31], the extent of reinforcement resulting from equation (2.6) can lead to a higher demand for punching shear reinforcement with respect to ETA procedure.

3. New procedure in the light of experimental investigations

The new design procedure was verified on the basis of experimental results of a total of more than 300 elements included in databases (among others [32,33]) corresponding to slender slabs, foundation slabs and footings, loaded in an axial and eccentric manner. For flat slabs without punching shear reinforcement, an average ratio of experimental to theoretical load capacity of about 1.10 was obtained with a coefficient of variation of about 12%. Importantly, the predictions did not show any noticeable trend, unlike the previous approach [26], affected by column size-to-effective depth ratio and effective depth of the member (scale effect) [34]. Good agreement was also achieved for flat slabs with punching shear reinforcement, yielding an average V_{exp}/V_{calc} ratio of about 1.20 with a coefficient of variation of about 12%. At the same time, the prediction quality was not found to be dependent on any of the main parameters, such as effective depth, concrete compressive strength, slab slenderness, longitudinal or shear reinforcement ratio.

An interesting aspect of predicting the punching resistance also seems to be the verification of the failure mode, which, in the case of shear-reinforced slabs, can be associated with the formation of a diagonal crack within the shear-reinforced area ($V_{Rd,cs}$) or outside it ($V_{Rd,out}$) but also with exceeding the effective strength of concrete within the direct connection to the column ($V_{Rd,max}$). For this reason, it was decided to analyse the results of the experimental investigations on flat slabs that were not included in the databases, previously cited. The comparison includes also slab with a deliberately introduced installation error, resulting in a reduction in the effective depth by 20% with respect to the designed value.

3.1. Characterisation of the test specimens

A comparison of the theoretical punching load capacities was carried out to evaluate the procedure [21] in the light of previous approach [26], including the results of experimental investigations carried out at the Lodz University of Technology [35, 36]. They included specimens with dimensions of $2.3 \times 2.3 \times 0.18$ m, reflecting the internal column-and-slab connection. The research program covered three series. In the first (S), the columns had a square cross-section with a side length $c = 0.25$ m, while in the other two (P and PM), they had a circular cross-section with a diameter of $D = 0.25$ m. The elements were made of concrete with an average compressive strength of $f_{cm} = 14.9 \div 45.3$ MPa and reinforcing steel with a yield strength of $f_{ym} = 517.9 \div 585.1$ MPa. The upper reinforcement mesh consisted of bars ∅12 every 150 mm or ∅6 every 90 mm ($\rho_1 = 0.51$ and 1.53‰), for the S, P and PM-series specimens, respectively. The cover of top reinforcement was $c_{nom} = 15 \div 20$ mm, except for element S4, where it was increased to 50 mm to account for the effect of a typical execution error of lowering the reinforcement under on-site conditions. Bottom reinforcement consisted of ∅8 every 150 mm and ∅10 every 180 mm, for the S, P and PM-series specimens, respectively. Most of the elements of the second and third series contained transverse reinforcement in the form of double-headed studs with a diameter of ∅12 ($A_{sw} = 118.8$ mm^2), arranged radially around the columns. The test specimens were presented on Figs. 9 and 10.

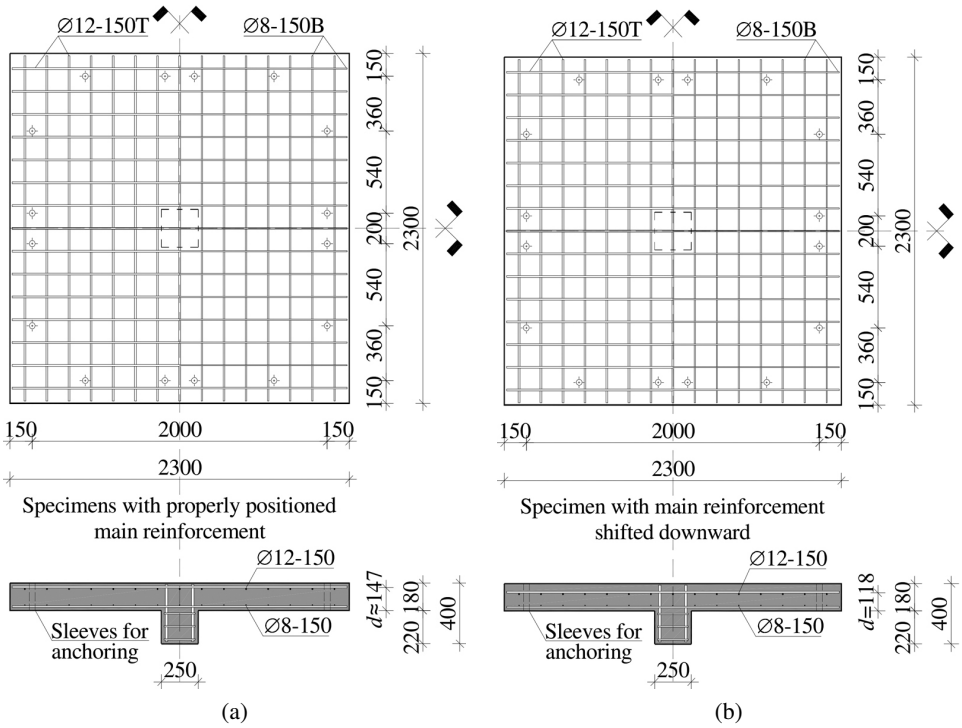

Fig. 9. Specimens: (a) S-1÷S-3, (b) S-4 from the tests [35]

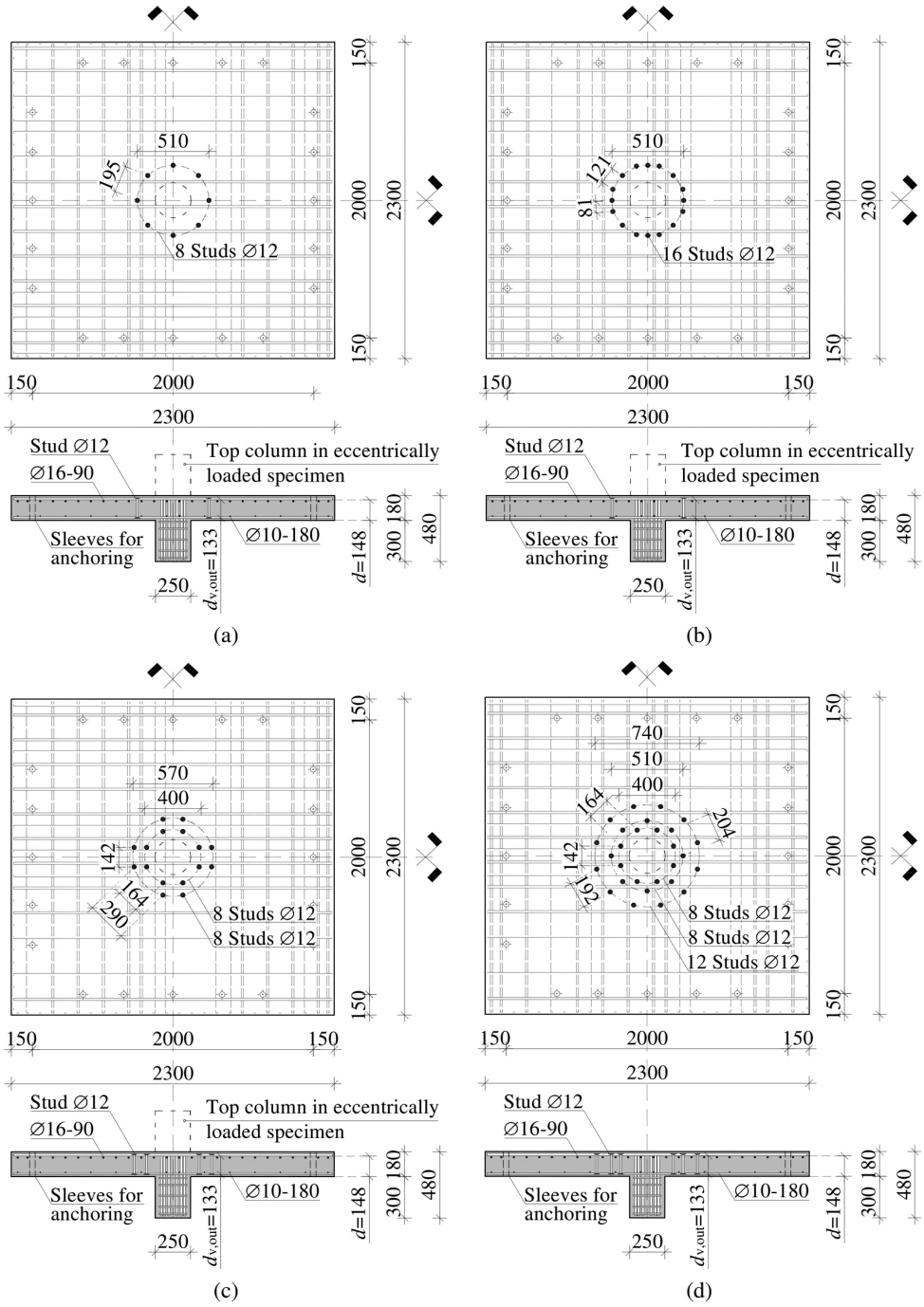

Fig. 10. Specimens: (a) P-8.1, P-8.1M, (b) P-16.1, P-16.1M, (c) P-16.2, P-16.2M, (d) P-28.3 [36]

The test setup allowed for fixing the slabs with 16 bolts placed evenly around the perimeter and enabled axial (S and M models) or eccentric (PM) load application on the columns. The load eccentricity for the PM models was fixed at $e = 0.1$ m. All the specimens were loaded gradually until failure.

3.2. Load capacities and failure modes

The new Eurocode EN 1992-1-1:2023 [21] allows for the iterative determination of punching shear resistance for individual reinforcement perimeters, which is important in engineering practice and allows for a more optimal slab design. The verification of the shear stresses is carried out at the control sections corresponding to location of the shear reinforcement. An iterative approach is used to find the shear force V_{Ed} at which the shear stress τ_{Ed} on the considered control perimeter reaches the punching shear resistance $\tau_{\mathrm{Rd,cs.}}$ The parameter β_{e}, which takes into account the non-uniform distribution of shear stresses, is estimated individually for each perimeter under consideration. In the case of a constant load eccentricity, the solution sought is reduced to solving an equation with one variable. A number of modifications are applied, including the following: using a reduced effective depth $d_{\mathrm{v,out}}$, replacing the control perimeters b_0 and $b_{0,5}$ with $b_{0,5,\mathrm{s}}$ (perimeter of the reinforcement) and $b_{0,\mathrm{s}}$ (perimeter moved $0.5d_{\mathrm{v,out}}$ away from it in the column direction), determining the punching shear resistance $\tau_{\mathrm{Rd,c}}$ for each of the sections under consideration (a factor k_{pb} is calculated in each case, depending on the lengths of the perimeters $b_{0,\mathrm{s}}$ and $b_{0,5,\mathrm{s}}$) adjusted by the factor $(d_{\mathrm{v}}/d_{\mathrm{v,out}})^{0,5}$ to account for reduced effective depth of the slab.

Table 1 summarises the theoretical load capacities for the experimental models S, P, PM, calculated on the basis of standards [21, 26] and the EOTA technical report TR 060 [37]. Although the standard [26] does not include the use of double-headed studs, the general design procedure for punching shear-reinforced members was used, assuming that the maximum stress at the control perimeter cannot exceed $V_{\mathrm{Rd,max}}(u_1) = 1.5\nu_{\mathrm{Rd,c}}$ – even though the reinforcement used did not meet the structural spacing requirements in some cases. For Eurocode EN1992-1-1:2023 [21], an iterative procedure for determining the punching resistance was used. Figure 11 compares the detailed load capacities of two selected elements (P-28.3, P-16.2M) resulting from the different failure mechanisms. All calculations were made considering the mean strength parameters determined by the tests ($\gamma_M = 1.0$).

An average ratio of experimental to theoretical capacities $V_{\mathrm{exp}}/V_{\mathrm{calc}}$ of 1.29, 1.32, 1.22 was obtained for the procedures presented in EN 1992-1-1:2004 [26], EOTA TR 060 [37] and EN 1992-1-1:2023 [21], respectively, with a coefficient of variation of 7÷14%. The theoretical load capacities $V_{\mathrm{R,c}}$ for elements without transverse reinforcement were found to be similar to those determined according to the other design approaches (differences not exceeding 11%). The calculations according to procedures [21, 26] indicated in almost all the specimens with shear reinforcement failure outside the punching shear-reinforced zone ($V_{\mathrm{R,out}}$). The procedure [37] requires for the transfer of the entire shear force via the doble-headed studs and, due to its limited number in the elements of the P-8 series, load capacities $V_{\mathrm{R,s}}$ turned out to be less than the load capacity $V_{\mathrm{R,c}}$. In other cases, the failure was due to exceeding the load capacity $V_{\mathrm{R,out}}$. According to the new edition of Eurocode 2 [21], the maximum load-carrying

Table 1. Comparative analysis of the punching shear capacities

Test specimen		f_{cm}	Eurocode 2:2004 [26]							EC2:2004+ETA			Eurocode 2:2023 [21]					
			V_{exp}	$V_{R,c}$	$V_{R,max}$	$V_{R,cs}$	$V_{R,out}$	V_{calc}	$\frac{V_{exp}}{V_{calc}}$	$V_{R,s}$	V_{calc}	$\frac{V_{exp}}{V_{calc}}$	$V_{R,c}$	$V_{R,max}$	$V_{R,cs}$	$V_{R,out}$	V_{calc}	$\frac{V_{exp}}{V_{calc}}$
		[MPa]	[kN]	[kN]	[kN]	[kN]	[kN]	[kN]		[kN]	[kN]		[kN]	[kN]	[kN]	[kN]	[kN]	
[35]	S-1	45.3	500	**428**	–	–	–	428	1.17	–	428	1.17	**446**	–	–	–	446	1.12
	S-2	38.8	495	**399**	–	–	–	399	1.24	–	399	1.24	**417**	–	–	–	417	1.19
	S-3	38.9	475	**406**	–	–	–	406	1.17	–	406	1.17	**423**	–	–	–	423	1.12
	S-4	40.2	367	**311**	–	–	–	311	1.18	–	311	1.18	**346**	–	–	–	346	1.06
[36]	P-0	19.2	495	**435**	–	–	–	435	1.14	–	435	1.14	**405**	–	–	–	405	1.22
	P-8.1	30.0	750	505	736	844	**564**	564	1.33	350	505	1.49	507	839	700	**590**	590	1.27
	P-16.1	25.2	700	478	639	1290	**540**	540	1.30	700	540	1.30	467	774	868	**562**	562	1.25
	P-16.2	24.7	700	473	621	1067	**559**	559	1.25	700	559	1.25	460	762	593	**576**	576	1.22
	P-28.3	14.9	675	400	**391**	1083	558	391	1.73	700	391	1.73	357	592	**545**	547	545	1.24
	P-0M	24.3	425	**384**	–	–	–	384	1.11	–	384	1.11	**357**	–	–	–	357	1.19
	P-8.1M	28.6	625	406	577	685	**453**	453	1.38	286	406	1.54	388	642	565	**493**	493	1.27
	P-16.1M	20.6	575	364	431	1034	**411**	411	1.40	572	411	1.40	329	545	688	**447**	447	1.29
	P-16.2M	25.7	650	392	526	876	**463**	463	1.40	572	463	1.40	367	609	**467**	501	467	1.39
							Mean:	1.29						1.32				1.22
							COV:	0.13						0.14				0.07

capacities $V_{R,max}$ calculated on the basic control perimeter were, on average, 5% higher than those derived from the previous standard [26]. In contrast, when compared to the EOTA approach [37], the values were 20% lower, which was attributed to the higher value of the

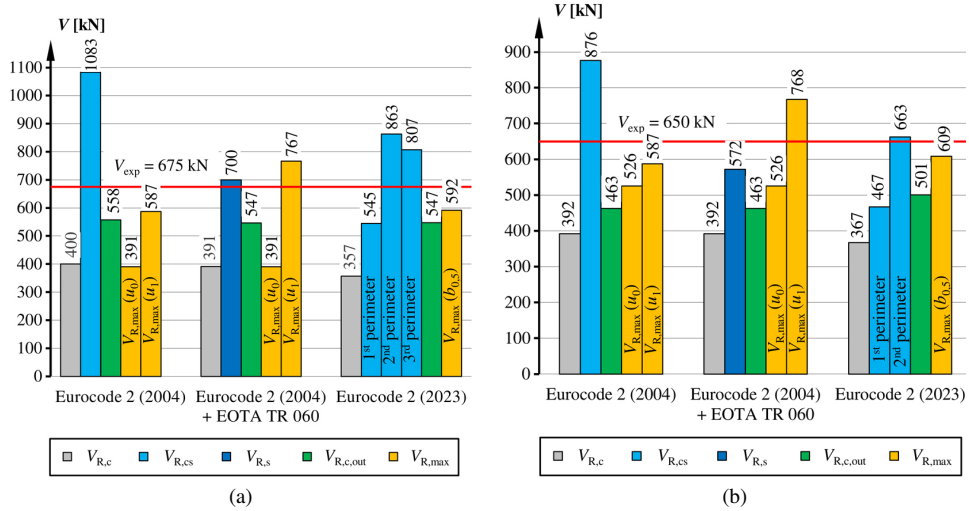

Fig. 11. Theoretical load carrying capacities of the test specimens: (a) P-28.3, (b) P-16.2M

coefficient $k_{max} = 1.96$. Notably, the new design procedure [21] does not include the check for $V_{R,max}$ load capacity at the edge of the supporting area, a criterion that was more restrictive for the considered specimens (especially for slab P-28.3). The failure of the P-16 and P-28 series elements was associated with the formation of a diagonal crack outside the shear-reinforcement zone. Only in the case of the P-8 specimens shear crack crossed the transverse reinforcement and was inclined at an angle of 30° [36]. Despite the reinforcement spacing requirements not being met in most of the analysed specimens, failure within the reinforced zone was observed in only two models. Similar to [26], the new procedure correctly identified the failure mechanism in only a few cases. However, it is worth noting the relatively small difference between the load carrying capacities $V_{R,cs}$ and $V_{R,out}$.

4. Conclusions and outlook

The new edition of Eurocode 2 [21] has introduced many expected changes in the punching shear design of reinforced concrete slabs. The analysis demonstrated, that the predictions of the new standard are less conservative and provides the best agreement with the experimental results among all of the considered approaches ($V_{exp}/V_{calc} = 1.22$, with a COV of 7%). Importantly, the predictions remained safe, even though the reinforcement of some elements did not meet the design requirements in terms of spacing or the number of the perimeters of shear reinforcement.

Acknowledgements

The paper has been completed while the second author was the Doctoral Candidate in the Interdisciplinary Doctoral School at the Lodz University of Technology, Poland.

References

[1] P.M. Lewiński and P.P. Więch, "Finite element model and test results for punching shear failure of RC slabs", *Archives of Civil and Mechanical Engineering*, vol. 20, no. 2, pp. 1–16, 2020, doi: 10.1007/s43452-020-00037-x.

[2] L. Buda-Ożóg, J. Zięba, K. Sieńkowska, and D. Nykiel, "Influence of the tie reinforcement on the development of a collapse caused by the failure of an edge column in RC flat slab system", *Archives of Civil Engineering*, vol. 69, no. 1, pp. 39–54, 2023, doi: 10.24425/ace.2023.144158.

[3] M. Grabski and A. Ambroziak, "Experimental and analytical analysis of punching shear in flat slabs supported on column topped with concrete head", *Construction and Building Materials*, vol. 364, art. no. 129961, 2023, doi: 10.1016/j.conbuildmat.2022.129961.

[4] A. Ambroziak and M. Grabski, "Verification of punching shear outside the shear cap by the direct method", *Archives of Civil Engineering*, vol. 68, no. 4, pp.359–375, 2022, doi: 10.24425/ace.2022.143043.

[5] T. Urban, M. Gołdyn, J. Krakowski, and Ł. Krawczyk, "Experimental Investigation on Punching Behavior of Thick Reinforced Concrete Slabs", *Archives of Civil Engineering*, vol. 59, no. 2, 2013, doi: 10.2478/ace-2013-0008.

[6] A. Muttoni, "Punching shear strength of reinforced concrete slabs without transverse reinforcement", *ACI Structural Journal*, vol. 105, no. 4, pp. 440–450, 2008, doi: 10.14359/19858.

[7] M.F. Ruiz and A. Muttoni, "Applications of critical shear crack theory to punching of reinforced concrete slabs with transverse reinforcement", *ACI Structural Journal*, vol. 106, no. 4, pp. 485–494, 2009, doi: 10.14359/56614.

[8] A. Muttoni, J.T. Simões, D.M.V. Faria, and M.F. Ruiz, „A Mechanical Approach for the Punching Shear Provisions in the Second Generation of Eurocode 2", *Hormigon y Acero*, vol. 74, no. 299–300, pp. 61–77, 2023, doi: 10.33586/hya.2022.3091.

[9] C. Siburg, M. Ricker, and J. Hegger, "Punching shear design of footings: Critical review of different code provisions", *Structural Concrete*, vol. 15, no. 4, pp. 497–508, 2014, doi: 10.1002/suco.201300092.

[10] J. Einpaul, F. Brantschen, M. Fernández Ruizm and A. Muttoni, „Performance of punching shear reinforcement under gravity loading: Influence of type and detailing", *ACI Structural Journal*, vol. 113, no. 4, pp. 827–838, 2016, doi: 10.14359/51688630.

[11] R. Beutel and J. Hegger, "The effect of anchorage on the effectiveness of the shear reinforcement in the punching zone", *Cement and Concrete Composites*, vol. 24, no. 6, pp. 539–549, 2002, doi: 10.1016/S0958-9465(01)00070-1.

[12] M. Fernández Ruiz and A. Muttoni, "Size effect in shear and punching shear failures of concrete members without transverse reinforcement: Differences between statically determinate members and redundant structures", *Structural Concrete*, vol. 19, no. 1, pp. 65–75, 2018, doi: 10.1002/suco.201700059.

[13] D. Abu-Salma, R.L. Vollum, and L. Macorini, "Design of biaxially loaded external slab column connections", *Engineering Structures*, vol. 249, 2021, doi:10.1016/j.engstruct.2021.113326.

[14] F. Brantschen, D.M.V. Faria, M. Fernández Ruiz, and A. Muttoni, „Bond behaviour of straight, hooked, U-shaped and headed barsin cracked concrete", *Structural Concrete*, vol. 17, no. 5, pp. 799–810, 2016, doi:10.1002/suco.201500199.

[15] A. Muttoni and J. Schwartz, "Behaviour of beams and punching in slabs without shear reinforcement", in *IABSE Colloquium*. 1991, vol. 62, pp. 703–708.

[16] A. Muttoni, M.F. Ruiz, E. Bentz, S. Foster, and V. Sigrist, "Background to fib Model Code 2010 shear provisions – Part II: Punching shear", *Structural Concrete*, vol. 14, no. 3, pp. 204–214, 2013, doi:10.1002/suco.201200064.

[17] M. Gołdyn, "Application of the Critical Shear Crack Theory for calculation of the punching shear capacity of lightweight aggregate concrete slabs", *Archives of Civil Engineering*, vol. 69, no. 1, pp. 55–70, 2023, doi:10.24425/ace.2023.144159.

[18] M. Gołdyn and T. Urban, "UHPFRC hidden capitals as an alternative method for increasing punching shear resistance of LWAC flat slabs", *Engineering Structures*, vol. 271, art. no. 114906, pp. 1–18, 2022, doi:10.1016/j.engstruct.2022.114906.

[19] A. Muttoni, "Schubfestigkeit und Durchstanzen von Platten ohne Querkraftbewehrung (Shear capacity and punching shear of slabs without shear reinforcement)", *Beton- und Stahlbetonbau*, vol. 98, no. 2, pp. 74–84, 2003, doi: 10.1002/best.200300400.

[20] *Model Code 2010 – Final draft*, vol. 2. FIB, 2012.

[21] EN 1992-1-1:2023 Eurocode 2 – Design of concrete structures – Part 1–1: General rules and rules for buildings, bridges and civil engineering structures. CEN, 2023.

[22] SIA 262:2003 Concrete Structures, SIA, 2003.

[23] ACI 318-25 Building Code for Structural Concrete- Code Requirements and Commentary (ACI 318-25). ACI, 2025.

[24] A. Muttoni, M. Fernández Ruiz, and J. Simões, "Recent improvements of the Critical Shear Crack Theory for punching shear design and its simplification for code provisions", presented at fib Congress 2018 Better, Smarter, Stronger, 2018.

[25] A. Muttoni and M. Fernández Ruiz, "The Critical Shear Crack Theory for punching design: From a mechanical model to closed-form design expressions", in *fib Bulletin 81. Punching shear of structural concrete slabs* FIB, 2017, pp. 237–252, doi: 10.35789/fib.BULL.0081.Ch12.

[26] EN 1992-1-1:2004 Eurocode 2: Design of concrete structures – Part 1–1: General rules and rules for buildings. CEN, 2004.

[27] M. Gołdyn and T. Urban, "Komentarz do zasad obliczania płyt na przebicie w strefie słupów narożnych według Eurokodu 2 (Commentary on design provisions for punching shear at corner columns according to Eurocode 2)", *Journal of Civil Engineering, Environment and Architecture*, vol. 64, no. 3, pp. 235–245, 2017, doi:10.7862/rb.2017.118.

[28] M. Gołdyn and T. Urban, "Effect of load level of corner columns on punching shear resistance of flat slabs", *Budownictwo i Architektura*, vol. 19, no. 3, pp. 41–51, 2020, doi: 10.35784/bud-arch.2123.

[29] D.H. Fraile, J.T. Simões, M.F. Ruiz, and A. Muttoni, "A mechanical approach for the maximum punching resistance of shear-reinforced slab-column connections", in *fib Symposium.* 2021, pp. 1628–1639.

[30] M. Ricker and F. Häusler, "Europäische Bemessungsregeln für Doppelkopfanker als Durchstanzbewehrung (European design provisions for double headed studs as punching shear reinforcement)", *Beton- und Stahlbetonbau*, vol. 109, no. 1, pp. 30–42, 2014, doi: 10.1002/best.201300056.

[31] T. Urban and M. Gołdyn, "Projektowanie zbrojenia na przebicie płyt żelbetowych w świetle znowelizowanego Eurokodu 2 (Design of punching shear reinforcement in reinforced concrete slabs in light of the revised Eurocode 2)", *Inżynieria i Budownictwo*, 2025 (submitted for publication).

[32] A. Muttoni, M. Fernández Ruiz, and J.T. Simões, "The theoretical principles of the critical shear crack theory for punching shear failures and derivation of consistent closed-form design expressions", *Structural Concrete*, vol. 19, no. 1, pp. 174–190, 2018, doi: 10.1002/suco.201700088.

[33] R. Walkner, "Kritische Analyse des Durchstanznachweises nach EC2 und Verbesserung des Bemessungsansatzes (Critical review of EC 2 regarding punching and improving the design approach)", Innsbruck University, 2014.

[34] D. Kueres, C. Siburg, M. Herbrand, M. Classen, and J. Hegger, "Uniform Design Method for punching shear in flat slabs and column bases", *Engineering Structures*, vol. 136, pp. 149–164, 2017, doi:10.1016/j.engstruct.2016.12.064.

[35] T. Urban, M. Sitnicki, and J. Tarka, *Badania połączeń płyta – słup wzmacnianych zewnętrznie na przebicie (Investigations on column-and-slab connection externally strengthened)*. Katedra Budownictwa Betonowego, Politechnika Łódzka, 2010.

[36] T. Urban and M. Sitnicki, "Badania podparcia żelbetowej płyty na słupie, wzmocnionej zbrojeniem poprzecznym BAUMA (Investigation of the support of a reinforced concrete slab on a column, strengthened with transverse reinforcement BAUMA)", *Inżynieria i Budownictwo*, vol. 59, no. 9, pp. 527–533, 2003.

[37] EOTA, "Increase of punching shear resistance of flat slabs or footings and ground slabs – double headed studs – Calculation Methods. TR 060", 2017.

EN 1992-1-1:2023 – nowe spojrzenie na problem przebicia w żelbecie

Słowa kluczowe: przebicie, płyty żelbetowe, obwód kontrolny, zbrojenie poprzeczne, Eurokod 2

Streszczenie:

Nowe wydanie Eurokodu 2 (EN 1992-1-1:2023) wprowadziło istotne i długo wyczekiwane zmiany w projektowaniu konstrukcji żelbetowych. Na podstawie wyników badań i prac analitycznych rozszerzono oraz uszczegółowiono zasady dotyczące wymiarowania stref podporowych stropów płaskich. W celu opisania zjawiska przebicia wykorzystano model mechaniczny bazujący na Teorii Krytycznej Rysy Ukośnej (Critical Shear Crack Theory – CSCT), opracowanej i rozwijanej przez zespółpod kierunkiem Muttoniego. W porównaniu do procedury obliczeniowej przedstawionej w prenormie *fib* Model Code 2010 w nowym podejściu zrezygnowano z koncepcji kolejnych poziomów aproksymacji kąta obrotu płyty ψ, zastępując je gotowymi formułami obliczeniowymi. W stosunku do Eurokodu 2 (EN 1992-1-1:2004) zmodyfikowano położenie podstawowego obwodu kontrolnego, ustalając go w odległości $0,5d_{\mathrm{v}}$, zamiast $2d$ od krawędzi słupa. Ujednolicono także zasady dotyczące płyt smukłych i fundamentów, rezygnując z podejścia iteracyjnego i przyjmując, że rysa formuje się pod kątem 45°. Rozróżniono także wysokości użyteczne uwzględniane w analizie zginania (d) oraz przebicia (d_{v} i $d_{\mathrm{v,out}}$), przy czym wysokość $d_{\mathrm{v,out}}$ powiązano z rodzajem i sposobem kotwienia zbrojenia poprzecznego. Jednym z nowych parametrów przy obliczaniu nośności na przebicie stałsię rozmiar ziarna kruszywa, który determinuje mechanizm zazębiania kruszywa i wpływa na sposób przekazywania sił ścinających. Dodatkowo, wprowadzono parametr k_{pb}, który uwzględnia przejście z płaskiego na przestrzenne ścinanie, łącząc naprężenia

graniczne z kształtem i wielkością podpory, a także wysokością użyteczną płyty. W artykule dokonano oceny wprowadzonych zmian na naośność na przebicie płaskich płyt żelbetowych. W przypadku podpór o przekroju prostokątnym stwierdzono zwiększającą się różnicę pomiędzy teoretycznymi nośnościami na przebicie, określonymi według regułdotychczasowego i nowego Eurokodu 2, która, w zależności od stosunku wysokości użytecznej do szerokości słu. pa wynosiła od 5 do nawet 30%. W przypadku podpór o przekroju kołowym nośności obliczone według nowego Eurokodu 2 były o $8 \div 10\%$ niższe, niezależnie od omawianej relacji. Kolejną ważną i pożądaną zmianą było wprowadzenie nowej formuły do wyznaczania współczynnika zwiększającego β, odpowiadającego za koncentrację naprężeń stycznych wynikających z działania momentu niezrównoważonego przekazywanego z płyty na słup. Jak pokazały wcześniejsze analizy, przewidywania dotychczasowego Eurokodu 2 prowadziły do znacznego niedoszacowania nośności, nawet o 50%. Analiza wpływu tego parametru przeprowadzona dla podpór krawędziowych i narożnych wykazała, że nowy sposób wyznaczania parametru β_e, zaproponowany przez Volluma i in., prowadzi do nośności o 5 do 50% większych niż te uzyskiwane na podstawie procedury obliczeniowej z 2004 roku. W przeciwieństwie do normy EN 1992-1-1:2004, w nowym podejściu zakłada się zmienny udział betonu i zbrojenia poprzecznego w nośności na przebicie, co wynika z rzeczywistego zachowania płyty żelbetowej podczas obciążania. Wraz ze wzrostem deformacji i związanego z tym zarysowania należy oczekiwać zmniejszającego się udziału betonu, przy jednocześnie zwiększającym się udziale zbrojenia. Zrezygnowano ze stałej wartości współczynnika wyrażającego nośność maksymalną, uzależniając ją od szeregu parametrów, takich jak: rodzaj zastosowanego zbrojenia na przebicie, wielkość podpory czy wysokość użyteczna płyty. W przypadku trzpieni dwugłówkowych ograniczono możliwość zwiększenia nośności na przebicie o około $10 \div 15\%$ w porównaniu do procedury ETA ($k_{\max} = 1,96$). W pracy dokonano oceny nowej procedury normowej w świetle wyników badań eksperymentalnych prowadzonych na Politechnice Łódzkiej. Teoretyczne nośności określono zgodnie z procedurami EN 1992-1-1:2023, EN 1992-1-1:2004 oraz raportem technicznym EOTA TR 060. Rozważono trzynaście modeli, zgrupowanych w trzech seriach badawczych, obejmujących połączenia wewnętrzne płyt żelbetowych grubości 0,18 m i wymiarach w rzucie $2,3 \times 2,3$ m, oraz słupów o przekroju kołowym i kwadratowym. Elementy wykonano z betonu o średniej wytrzymałości na ściskanie $f_{\mathrm{cm}} = 14,9 \div 45,3$ MPa, zaś stopień zbrojenia głównego wynosił $\rho_{\mathrm{l}} = 0.51$ i 1.53%. Wybrane płyty zostały dodatkowo zazbrojone na ścinanie trzpieniami dwugłówkowymi $\varnothing 12$, rozmieszczonymi na jednym, dwóch lub trzech obwodach wokółsłupa. Elementy obciążano zarówno osiowo jak i ze stałym mimośrodem wynoszącym $e = 0,1$ m. Uzyskano średni stosunek nośności eksperymentalnej do teoretycznej równy 1,29, 1,32, 1,22, odpowiednio w przypadku procedur obliczeniowych EN 1992-1-1:2004, EOTA TR 060 oraz EN 1992-1-1:2023, przy współczynniku zmienności na poziomie $7 \div 14\%$. Nośności teoretyczne elementów bez zbrojenia na przebicie, wyznaczone dla wszystkich rozpatrywanych podejść obliczeniowych, były zbliżone, a różnice między nimi nie przekroczyły 11%. Należy zauważyć, iż przewidywania normy EN 1992-1-1:2023 okazały się bezpieczne, mimo iż zbrojenie niektórych elementów nie spełniało warunków konstrukcyjnych w zakresie rozstawu czy liczby obwodów. Obliczenia według tej procedury charakteryzowały się przy tym najlepszą zgodnością z wynikami badań eksperymentalnych ($V_{\mathrm{exp}}/V_{\mathrm{calc}} = 1,22$, $\alpha = 7\%$), zarówno w przypadku elementów bez zbrojenia jak i zbrojonych na przebicie. Nie we wszystkich przypadkach możliwe było oszacowanie prawidłowego sposobu zniszczenia, jednak podkreślenia wymaga stosunkowo nieduża różnica pomiędzy nośnościami powiązanymi z zewnętrznym przekrojem kontrolnym ($V_{\mathrm{R,out}}$) i strefą zbrojoną na przebicie ($V_{\mathrm{R,cs}}$). Warto zauważyć, iż podobny poziom zgodności nośności eksperymentalnych i teoretycznych uzyskano w przypadku elementów obciążonych osiowo i mimośrodowo, co potwierdziło prawidłowość nowej procedury określania wpływu niezrównoważonego momentu zginającego.

Received: 2025-05-28, Revised: 2025-06-13